Journal of Cell Science 112, 3373-3384 (1999)
Printed in Great Britain © The Company of Biologists Limited 1999
JCS4672

Glycogen synthase kinase 3β phosphorylation of microtubule-associated protein 1B regulates the stability of microtubules in growth cones

Robert G. Goold, Rebecca Owen and Phillip R. Gordon-Weeks*

Developmental Biology Research Centre, The Randall Institute, King's College London, 26-29 Drury Lane, London WC2B 5RL, UK
*Author for correspondence (e-mail: phillip.gordon-weeks@kcl.ac.uk)

Accepted 14 July; published on WWW 22 September 1999

SUMMARY

We have recently shown that glycogen synthase kinase 3β (GSK3β) phosphorylates the microtubule-associated protein (MAP) 1B in an in vitro kinase assay and in cultured cerebellar granule cells. Mapping studies identified a region of MAP1B high in serine-proline motifs that is phosphorylated by GSK3β. Here we show that COS cells, transiently transfected with both MAP1B and GSK3β, express high levels of the phosphorylated isoform of MAP1B (MAP1B-P) generated by GSK3β. To investigate effects of MAP1B-P on microtubule dynamics, double transfected cells were labelled with antibodies to tyrosinated and detyrosinated tubulin markers for stable and unstable microtubules. This showed that high levels of MAP1B-P expression are associated with the loss of a population of detyrosinated microtubules in these cells. Transfection with MAP1B protected microtubules in COS cells against nocodazole depolymerisation, confirming previous studies. However, this protective effect was greatly reduced in cells containing high levels of MAP1B-P following transfection with both MAP1B and GSK3β. Since we also found that MAP1B binds to tyrosinated, but not to detyrosinated, microtubules in transfected cells, we propose that MAP1B-P prevents tubulin detyrosination and subsequent conversion of unstable to stable microtubules and that this involves binding of MAP1B-P to unstable microtubules. The highest levels of MAP1B-P are found in neuronal growth cones and therefore our findings suggest that a primary role of MAP1B-P in growing axons may be to maintain growth cone microtubules in a dynamically unstable state, a known requirement of growth cone microtubules during pathfinding. To test this prediction, we reduced the levels of MAP1B-P in neuronal growth cones of dorsal root ganglion cells in culture by inhibiting GSK3β with lithium. In confirmation of the proposed role of MAP1B-P in maintaining microtubule dynamics we found that lithium treatment dramatically increased the numbers of stable (detyrosinated) microtubules in the growth cones of these neurons.

Key words: MAP1B, Growth cone, GSK3β, Proline-directed kinase, Microtubule, Axonogenesis

INTRODUCTION

The microtubule-associated protein (MAP) 1B is a developmentally regulated phosphoprotein that is expressed at high levels in growing neurons and in regions of the adult nervous system that show neuronal plasticity or regenerate after injury (reviewed by Müller et al., 1994). Although the precise function of MAP 1B is unclear, indirect evidence strongly suggests that the molecule plays an important role in axon growth and possibly in growth cone structure and dynamics (reviewed by Gordon-Weeks, 1997). For example, it is the first structural MAP to be expressed in developing neurons (Tucker et al., 1988) and the expression is particularly high in growing axons and their growth cones (Bloom et al., 1985; Calvert and Anderton, 1985; Riederer et al., 1986; Schoenfeld et al., 1989; Fischer and Romano-Clarke, 1991; Mansfield et al., 1991; Gordon-Weeks et al., 1993). Inhibition of expression with antisense oligodeoxynucleotides blocks neurite growth in PC12 cells (Brugg et al., 1993) and cerebellar macroneurons (DiTella et al., 1996). More recently, two transgenic MAP 1B 'knockout' mice have been produced (Edelmann et al., 1996; Takei et al., 1997). In the Edelmann et al. (1996) knockout the homozygotes die in utero and the heterozygotes show widespread neurological disorders (Edelmann et al., 1996). In contrast, in the second knockout, homozygous mice survive and show only a delay in the development of their nervous systems (Takei et al., 1997). However, these animals may not be complete knockouts since there is evidence that they express a truncated isoform of MAP1B, at low levels (Takei et al., 1997). Furthermore, analysis of the MAP1B gene in mice and rats predicts that truncated transforms exist in the Takei et al. (1997) knockout (Kutschera et al., 1998).

There are two classes of phosphorylated isoforms of MAP1B; one is developmentally down-regulated, expressed only in growing axons and generated by proline-directed kinases, including the cyclin-dependent kinase cdk5 and glycogen synthase kinase 3β (GSK3β) (DiTella et al., 1996;

Lucas et al., 1998); the second isoform is expressed throughout the neuron, maintained into adulthood and probably generated by casein kinase II (Díaz-Nido et al., 1988; Ulloa et al., 1993a). The developmentally down-regulated phosphorylated isoforms are particularly concentrated in growth cones (Mansfield et al., 1991; Black et al., 1994; Bush and Gordon-Weeks, 1994; Bush et al., 1996; DiTella et al., 1996), an observation which further supports their role in axon growth.

Although the precise effect of phosphorylation on MAP 1B function is not known, there is some evidence that phosphorylated isoforms bind microtubules more effectively than non-phosphorylated isoforms (Brugg and Matus, 1988; Aletta et al., 1988; Díaz-Nido et al., 1988). The interaction of MAP 1B with actin filaments also appears to be regulated by phosphorylation, at least in vitro (Pedrotti and Islam, 1996). A number of monoclonal antibodies (mAbs) recognise developmentally regulated phosphorylation epitopes on MAP 1B including 1B6 (Sato-Yoshitake et al., 1989), 150 (Mansfield et al., 1991; Gordon-Weeks et al., 1993; Ulloa et al., 1993b), 1BP (Black et al., 1994), SMI-31 (Fischer and Romano-Clarke, 1990; Bush and Gordon-Weeks, 1994; Johnstone et al., 1997a) and RT97 (Johnstone et al., 1997b). These antibodies have proved useful in mapping the developmental expression of the different phosphorylated isoforms. We have recently identified the sites on MAP 1B recognised by mAb SMI-31 (Johnstone et al., 1997a). One of these is characterised by a remarkably high concentration of serines followed, immediately downstream, by a proline, suggesting that the kinase responsible is a proline-directed serine kinase. We have confirmed the involvement of a proline-directed serine kinase by showing that GSK3β phosphorylates MAP1B at sites recognised by mAb SMI-31 in an in vitro kinase assay and in cerebellar granule cells in culture (Lucas et al., 1998). In this report we have explored the effect that phosphorylation of MAP1B by GSK3β has on microtubule dynamics in transfected COS and CHO cells and in dorsal root ganglion neurons in culture. A preliminary report of part of this work in abstract form has already appeared (Goold and Gordon-Weeks, 1998).

MATERIALS AND METHODS

Transfection of COS and CHO cells

A full length mouse MAP1B cDNA cloned into the pSVsport vector (BRL) was obtained from Prof. N. Cowan (Noble et al., 1989). Human GSK3β cDNA cloned into the pMT-2 vector was a gift from Dr J. Woodgett (Lovestone et al., 1994). Plasmids were purified on CsCl gradients and used to express protein in COS-7 and CHO cells grown in DMEM (Gibco) containing 10% foetal bovine serum (Gibco) supplemented with 2 mM glutamine, 100 i.u. ml^{-1} penicillin and 100 i.u. ml^{-1} streptomycin. Cells (1×10^5 for COS-7 and 2×10^5 for CHO) were either plated onto 13 mm glass coverslips in 35 mm Petri dishes for immunofluorescence microscopy or directly onto plastic Petri dishes for biochemical analysis. Cells were transfected by lipofection using Lipofectamine reagent (Gibco BRL) and 2 μg DNA per dish according to the manufacturer's protocol. For double transfection experiments, an equal quantity of each plasmid was added simultaneously. For controls, cells were treated as for transfections except that DNA was omitted. Twenty fours hours after transfection was initiated the transfection medium was replaced with complete DMEM and the cells were harvested or fixed 24 hours later. At this time point, cultures were about 80% confluent. In some experiments, 20 mM LiCl or 20 mM NaCl was added with the complete medium.

To assay microtubule stability, nocodazole was added to the culture medium to a final concentration of 0.1 μg/ml (Piperno et al., 1987). The cells were incubated for 30 minutes at 37°C prior to fixation as described below.

Immunofluorescence staining of COS and CHO cells

Cells were washed once with phosphate buffered saline (PBS) at 37°C and then fixed in methanol at −20°C for 5 minutes and rehydrated in PBS. In some cases, soluble cellular protein was extracted for 5 minutes with PHEM buffer at 37°C (Schliwa and van Blerkom, 1981) containing 1% (v/v) Triton X-100 prior to fixation (Bush et al., 1996). Cells were stained as previously described (Bush et al., 1996) using the following antibodies: monoclonal antibodies against total MAP1B (R, diluted 1:10, Riederer et al., 1986), MAP1B phosphorylated by GSK3β (SMI-31, Affiniti, diluted 1:100), GSK3β (Affiniti, diluted 1:50), acetylated α-tubulin (6-11B-1, 1:2.5, Piperno and Fuller, 1985), tyrosinated α-tubulin (YL 1/2, Sera Lab, diluted 1:10) and TAT-1, a mouse mAb recognising all forms of α-tubulin (Woods et al, 1989, diluted 1:100) were used together with polyclonal antibodies (pAb) against total MAP1B (αMAP1B-C1, Johnstone et al., 1997b, diluted 1:100), and detyrosinated α-tubulin (SUP GLU, diluted 1:1000, Gundersen et al., 1984). Double labelling was done with appropriate Texas Red (Jackson ImmunoResearch), Alexa 488 and 568 (Molecular Probes) or fluorescein (Sigma)-conjugated secondary antibodies; in triple labelling experiments, Cy-5-conjugated secondary antibodies (Jackson ImmunoResearch) were included. Rat and mouse secondary antibodies had been preabsorbed against either rat or mouse serum, as appropriate. To control for non-specific binding, primary antibodies were excluded, and to control for cross-reactivity of secondary antibodies, a potential problem since we are using mouse and rat primary antibodies, combinations of inappropriate primary and secondary antibodies were assessed. All controls were negative or showed low background staining. Cultures were washed in PBS and mounted in Citifluor (Citifluor Ltd, City University) on microscope slides and viewed by phase-contrast or fluorescence optics using an Olympus BM2 microscope or a Leica TCS confocal microscope equipped with Argon, Krypton and HeNe lasers. In the confocal microscope, cells were imaged with a ×63/1.32 PLANAPO oil-immersion objective and recorded at 1024 × 1024 pixels per image. Switching off the appropriate laser line using the AOTF in the confocal microscope showed that there was negligible 'bleed-through' between channels. Complete 'z' series optical sections were collected and projected onto a single plane using Leica TCS software. Fluorescent images in TIFF format were manipulated using Adobe Photoshop and analysed using NIH ImagePC.

Cell counts

To determine the proportion of cells expressing GSK3β, MAP1B or MAP1B-P we labelled cells with mAbs GSK3β, R or SMI-31, respectively, and counted 300 cells, on average, from each of three separate experiments in double transfected cultures and in cultures transfected with GSK3β or MAP1B alone. Monoclonal antibody SMI-31 recognises MAP1B-P but also cross-reacts with an unidentified nuclear epitope in all COS and CHO cells, a property which allowed us to count total cell number.

To determine the proportion of cells lacking stable microtubules, we double labelled COS cell cultures with mAb YL 1/2 and pAb SUP GLU and counted 100 cells from one coverslip from each of six separate experiments (i.e. 600 cells in total) and scored cells for SUP GLU immunofluorescence. Cells undergoing cell division, as indicated by the presence of a mitotic spindle, were discounted.

Nocodazole treated COS cells transfected with MAP1B or MAP1B and GSK3β were double labelled with TAT-1, and αMAP1B-C1.

Cells expressing high levels of MAP1B were selected and their microtubule content examined. These were divided into three classes: background, medium or high microtubule numbers (examples can be seen in Fig. 5). One hundred cells from each of three separate experiments (300 in total) were counted for each transfection. The proportion of cells expressing MAP1B-P in each experiment was determined by double labelling duplicate coverslips with αMAP1B-C1 and SMI-31.

To measure the fluorescence intensity of immunostained transfected COS cells, a series of optical slices from the top to the bottom of individual cells at 1 μm intervals was obtained in the confocal microscope. Cells were selected for fluorescence measurements if they had moderate to high levels of MAP1B or MAP1B-P. Ten cells from each of three separate experiments from both MAP1B and MAP1B and GSK3β transfected cultures were measured. The total fluorescence from each fluorophore was determined using Leica TCS-NT software. For these measurements the AOTF, PMT and laser output settings were held constant. No correction was made for mAb SMI-31 nuclear staining or for background fluorescence, which we estimate to be less than 1%.

Biochemical analysis of COS cells

Transfected cells were washed once with PBS and scraped into hot sodium dodecyl sulphate polyacrylamide gel electrophoresis (SDS-PAGE) sample buffer. A high speed supernatant from neonatal mouse brain was used as an independent standard for MAP1B. Protein samples were subjected to SDS gradient (4-15%) gel electrophoresis using Laemmli (1970) buffers and western blotted onto nitrocellulose membrane according to the method of Towbin et al. (1979). Blots were immunolabelled as described (Johnstone et al., 1997a). Blots were developed with an ECL chemiluminescent kit (Pierce), scanned using a flat-bed scanner (Hewlett Packard ScanJet 4C) and analysed using Phoretix 1D Plus gel analysis software. Immunoblotting was done with the antibodies detailed above, using the following dilutions: R, diluted 1:500; SMI-31, diluted 1:500; anti-GSK3β, diluted 1:2000; TAT-1, diluted 1:1000; YL 1/2, diluted 1:40; 6-11B-1, diluted 1:20; SUP GLU, diluted 1:2000 and with a mixture of pAb ERK 1 and 2 antibodies (Santa Cruz, diluted 1:1000). To ensure equal protein loading, protein samples were assayed by densitometry of Coomassie blue stained gels and adjusted for blotting. To confirm equal protein loading, ERK1 and 2 immunoreactivity of blots was quantified by densitometry.

To separate cytosolic and cytoskeletal associated proteins, cells were washed once with PBS at 37°C, and were then extracted with PHEM buffer containing 1% Triton X-100 for 5 minutes at room temperature. The soluble (cytosolic) material was aspirated and prepared for SDS-PAGE. The insoluble material remaining attached to the dish was scraped into SDS-PAGE sample buffer. Equal proportions of each fraction, representing protein from the same number of cells, were analysed by western blotting.

Dorsal root ganglion cell culture

Early postnatal TO mice were anaesthetised by intra-peritoneal injection of Sagatal (pentobarbitone) and dorsal root ganglia were dissected under sterile conditions and cultured as described previously (Bush et al., 1996). Cells were plated at a density of $1\text{-}2\times10^4$ cells/cm^2 onto glass coverslips coated with poly-D-lysine (10 μg/ml, Sigma) and laminin (10 μg/ml, Sigma) for immunofluorescence analysis or at a density of 8.5×10^3 cells/cm^2 onto 35 mm dishes coated as described above for biochemical analysis. Cells were incubated in supplemented Ham's F-14 medium containing NGF (60 ng/ml, Sigma) in the presence of 10-20 mM LiCl or NaCl for 24 hours. Cultures were fixed with 3% (w/v) formaldehyde/0.2% (v/v) glutaraldehyde in PBS (pH 7.2) containing 0.2% Triton X-100 and 10 mM EGTA for 10 minutes at 37°C or scraped into hot SDS sample buffer as described for COS and CHO cells. To label actin we used mAb AC-15 (Sigma, 1:100) which recognises β-actin.

RESULTS

Transient transfection of COS and CHO cells with GSK3β and MAP1B leads to high levels of MAP1B-P expression

COS and CHO cell cultures were either double transfected with GSK3β and full-length MAP1B or with GSK3β or MAP1B alone. COS and CHO cell cultures treated as for transfected cells but without plasmid were used as controls. Immunofluorescence staining of non-transfected, control COS and CHO cells with antibodies to GSK3β, MAP1B and MAP1B-P showed that there were low levels of GSK3β and MAP1B in these cells but no appreciable amounts of MAP1B-P, as indicated by a lack of staining with mAb SMI-31 (not shown). This was confirmed by immunoblotting experiments (Fig. 1). When COS cell cultures were transfected with GSK3β alone, there was a high level of GSK3β expression in 36% (*n*=1763) of cells but no appreciable phosphorylation of the endogenous MAP1B to form the phosphorylated isoform recognised by mAb SMI-31 (MAP1B-P) (Fig. 1). When COS cell cultures were transfected with MAP1B alone, there was a high level of MAP1B expression in 35% (*n*=1789) of cells and, in some cells, the appearance of MAP1B-P, as indicated by mAb SMI-31 staining (not shown) and immunoblotting (Fig. 1). Immunofluorescence analysis of COS cell cultures stained with mAb SMI-31 showed that 7.6% (*n*=954) of cells

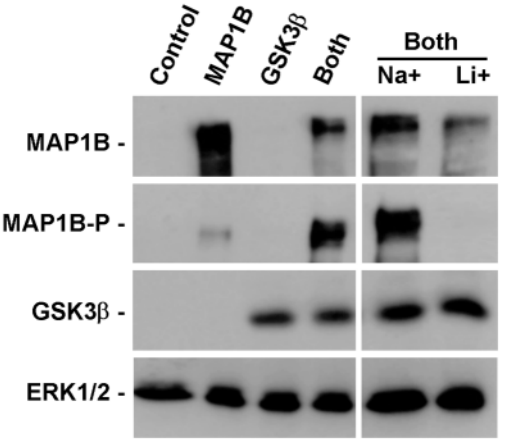

Fig. 1. COS cells double transfected with MAP1B and GSK3β express high levels of MAP1B-P. Whole cell extracts from controls (Control), MAP1B transfected (MAP1B), GSK3β transfected (GSK3β) and MAP1B and GSK3β transfected COS cells (BOTH) were prepared for SDS-PAGE and immunoblotting. Double transfected cells grown in the presence of NaCl (20 mM) or LiCl (20 mM) were also analysed (lanes Na^+ and Li^+). Blots were probed with antibodies to MAP1B (mAb R), MAP1B-P (mAb SMI-31), GSK3β and ERK1 and 2. This analysis confirmed the expression of MAP1B and GSK3β in transfected cells and shows that high levels of expression of MAP1B-P are produced only when cells are double transfected. Longer exposure of the film to these blots indicates that low levels of both MAP1B and GSK3β are expressed in COS cells. Note that MAP1B-P expression is inhibited specifically by LiCl and that only the lower band of MAP1B is present. Brain proteins from a high speed supernatant from neonatal rat brain were run in parallel as an independent marker for MAP1B (not shown). Blotting with ERK1 and 2 antibodies confirmed that protein loading was the same in each lane.

contained MAP1B-P in MAP1B transfections. In COS cell cultures double transfected with GSK3β and MAP1B, we found a much higher proportion of cells that contained MAP1B-P (34%; *n*=1,134), as indicated by mAb SMI-31 immunofluorescence (not shown) and immunoblotting (Fig. 1). MAP1B was present as a doublet in these cells (Fig. 1). Similar results were observed in transfected CHO cell cultures. The intensity of mAb SMI-31 staining of individual cells varied, suggesting that individual transfected cells express different levels of MAP1B-P. Immunoblotting analysis (Fig. 1) and immunofluorescence (not shown) showed that lithium, an inhibitor of GSK3β (Klein and Melton, 1996; Stambolic et al., 1996; Hedgepeth et al., 1997) prevented the phosphorylation of MAP1B in cultured COS cells double transfected with MAP1B and GSK3β. Only the lower band was present in immunoblots of lithium treated cells, consistent with the suggestion that phosphorylation of MAP1B causes a decrease in the mobility in SDS-PAGE (Ulloa et al., 1993b). These experiments confirm our previous finding that GSK3β phosphorylates MAP1B at a site recognised by mAb SMI-31 in an in vitro kinase assay and in cerebellar granule cells in culture (Johnstone et al., 1997a; Lucas et al., 1998).

MAP1B-P down-regulates detyrosinated microtubules in transfected COS and CHO cells

Phosphorylation of MAP1B is thought to regulate its interactions with microtubules and actin filaments (Brugg and Matus, 1988; Aletta et al., 1988; Díaz-Nido et al., 1988; Pedrotti and Islam, 1996). To assess the effect of phosphorylation of MAP1B by GSK3β on microtubule dynamics we examined the distribution of dynamically stable and unstable microtubules in COS and CHO cells double transfected with GSK3β and MAP1B using antibody markers. To mark unstable microtubules we used mAb YL 1/2, which recognises tyrosinated α-tubulin (Kilmartin et al., 1982; Wehland et al., 1984), and to mark stable microtubules, polyclonal antibody (pAb) SUP GLU, which binds to detyrosinated α-tubulin (Gundersen et al., 1984; Bulinski et al., 1988), and mAb 6-11B-1, which recognises acetylated α-tubulin (Piperno and Fuller, 1985). In control COS cell cultures, we found that all cells had a population of tyrosinated microtubules (YL 1/2$^+$) but that a small proportion of cells (7.8±3.5%, mean ± s.d., *n*=600) lacked detyrosinated microtubules (SUP GLU$^-$) (Fig. 2). The detyrosinated microtubules were characteristically curled, with loops and bends and were fewer in number than the tyrosinated microtubules, which tended to be straighter. Most cells had acetylated microtubules (mAb 6-11B-1$^+$, see Fig. 7C). In COS cell cultures double transfected with GSK3β and MAP1B, there was a significant increase in the proportion of cells without detyrosinated microtubules (27.5±7.2%, mean ± s.d., *n*=600; Fig. 2). A similar increase in the proportion of cells without detyrosinated microtubules was seen in transfected CHO cells (not shown). Transfection with either MAP1B or GSK3β alone caused a more modest increase in the proportion of cells without detyrosinated microtubules (Fig. 2). In double transfected COS cell cultures treated with lithium, there was no increase in the proportion of cells without detyrosinated microtubules (13±4.6%, mean ± s.d., *n*=300) compared to single transfections with either MAP1B or GSK3β (Fig. 2). To determine whether there was also a loss of acetylated microtubules in transfected cells we double labelled transfected cells with mAb 6-11B-1, which recognises acetylated microtubules (Piperno and Fuller, 1985), and pAb SUP GLU, to detect detyrosinated microtubules. In MAP1B transfected COS cell cultures, we found that 89% of SUP GLU$^-$ cells (*n*=300) contained acetylated microtubules, and in MAP1B and GSK3β transfected COS cell cultures, 88% of SUP GLU$^-$ cells (*n*=300) contained acetylated microtubules. Thus, MAP1B and MAP1B-P had no effect on the levels of acetylated microtubules. We found no evidence of enhanced microtubule bundling in cells expressing MAP1B (c.f. Noble et al., 1989; Takemura et al., 1992) or MAP1B-P.

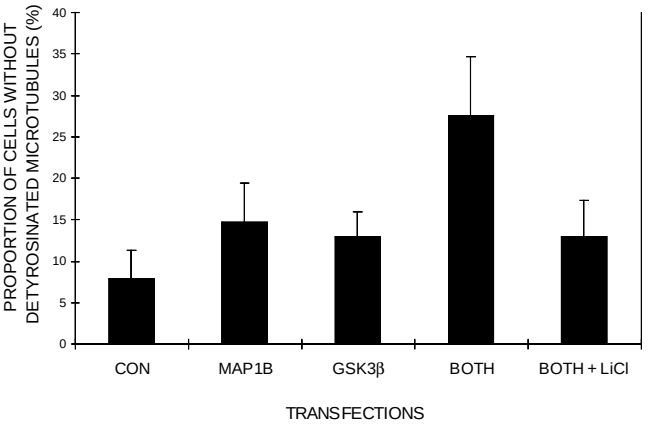

Fig. 2. Transfection of COS cells with MAP1B and GSK3β increases the proportion of cells without detyrosinated microtubules. Quantitative analysis of the proportion of COS cells completely lacking detyrosinated microtubules, as indicated by an absence of pAb SUP GLU staining, in control cultures (CON), cultures transfected with MAP1B, GSK3β, double transfected cultures (BOTH) or double transfected cultures treated with lithium chloride (BOTH + LiCl). Note that lithium treatment (BOTH + LiCl) partially reverses the effects of double transfection on detyrosinated microtubules. Values are means ± s.d. of 600 cells in each transfection category from 6 separate experiments.

To determine whether changes in detyrosinated microtubules correlated with the expression of MAP1B-P in these cells we triple labelled COS cell cultures double transfected with GSK3β and MAP1B with pAb SUP GLU, mAb YL 1/2 and mAb SMI-31. We found that in those cells expressing high levels of MAP1B-P there were no detyrosinated microtubules, as indicated by a lack of staining with pAb SUP GLU (Fig. 3A). When we double labelled MAP1B transfected cultures with pAb SUP GLU and an antibody that recognises all isoforms of MAP1B (mAb R) we found no correlation between high levels of MAP1B and lack of SUP GLU$^+$ microtubules (Fig. 3B). Since, in single, MAP1B transfected cultures, many cells express high levels of MAP1B but not GSK3β, and therefore low levels of MAP1B-P, it seems likely that the loss of detyrosinated microtubules in double transfected cultures is due to the presence of high levels of MAP1B-P, rather than MAP1B itself or GSK3β. Furthermore, in single transfections with either MAP1B or GSK3β, there are fewer cells without detyrosinated microtubules than in double transfections (Fig. 2). Consistent with this interpretation, lithium treatment of double transfected cells prevents the increase in the number of cells without detyrosinated microtubules. We confirmed the

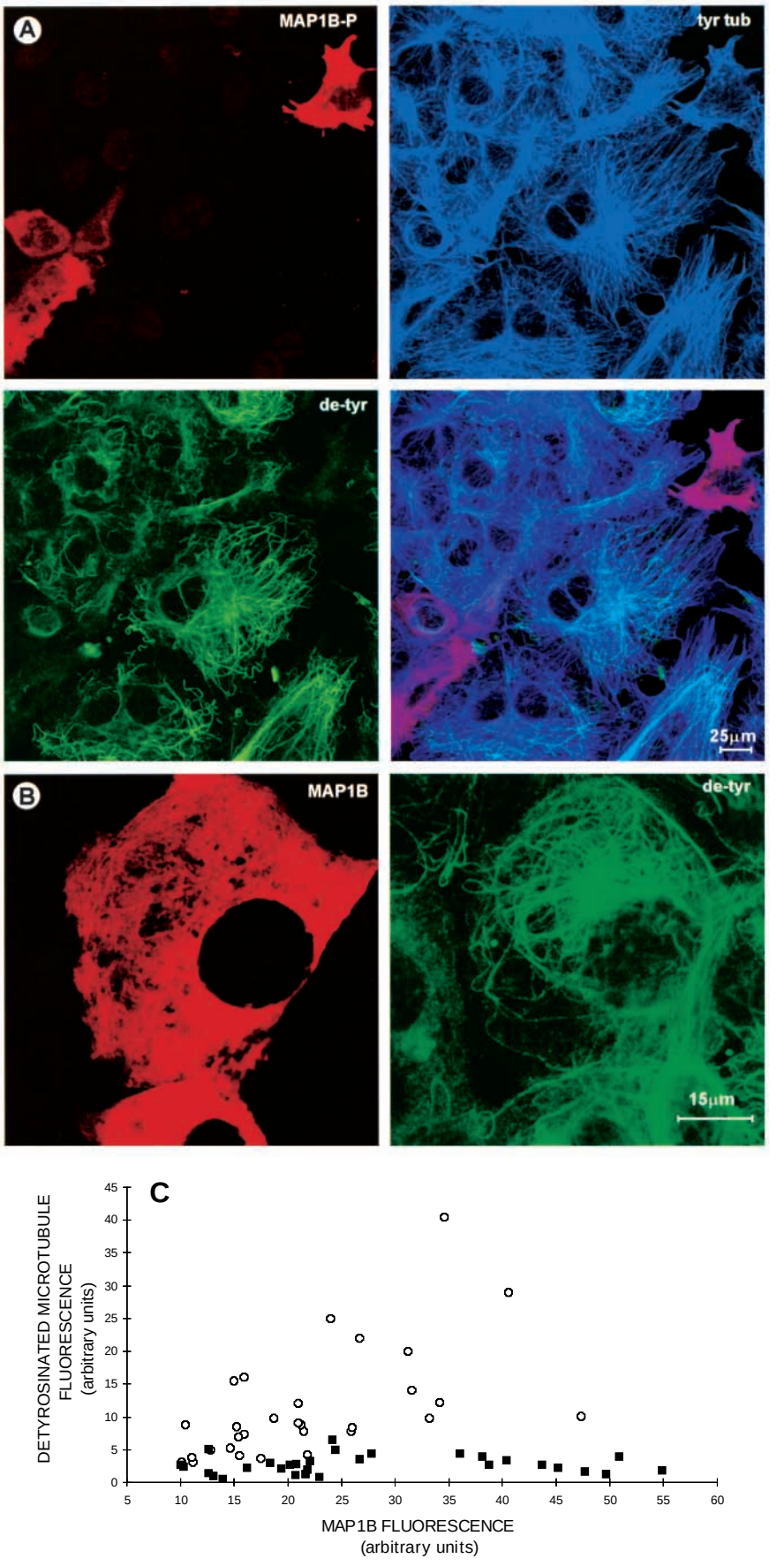

Fig. 3. (A)COS cells expressing high levels of MAP1B-P lack detyrosinated microtubules. Confocal fluorescence images of COS cells from cultures transfected with GSK3β and MAP1B and triple labelled with mAb SMI-31 (red) which recognises MAP1B-P, mAb YL 1/2 (blue), which labels tyrosinated microtubules, and pAb SUP GLU (green), which labels detyrosinated microtubules. Several cells in the field have high levels of MAP1B-P, as indicated by intense mAb SMI-31 staining, but either lack completely or have low numbers of detyrosinated microtubules. All of the other cells in the field do not express MAP1B-P but contain a normal complement of detyrosinated microtubules. All cells have tyrosinated microtubules. Note that in cells expressing high levels of MAP1B-P the microtubules are not noticeably more bundled than in cells not expressing MAP1B-P. mAb SMI-31 cross-reacts with a nuclear epitope in all COS cells. (B) COS cells expressing high levels of MAP1B may have a normal compliment of detyrosinated microtubules. COS cell cultures transfected with MAP1B were double labelled with mAb R (red), which recognises all forms of MAP1B, and pAb SUP GLU (green), which recognises detyrosinated microtubules.
(C) Moderate to high levels of MAP1B-P correlate with low levels of detyrosinated microtubules whereas there is no relationship between moderate to high levels of MAP1B and detyrosinated microtubules. Scatter plots showing the relationship between the amount of fluorescence due to pAb SUP GLU staining (detyrosinated microtubules) and mAb R (MAP1B, circles) or mAb SMI-31 (MAP1B-P, squares) staining in individual COS cells expressing high to moderate levels of either MAP1B (circles) or MAP1B-P (squares) from cultures transfected with MAP1B alone (circles) or MAP1B and GSK3β (squares).

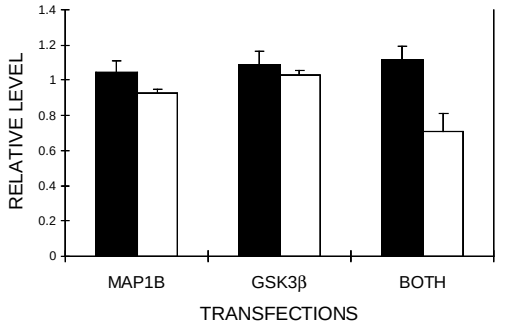

Fig. 4. MAP1B-P decreases the levels of detyrosinated tubulin. Quantitative immunoblotting analysis of the relative levels of tyrosinated tubulin (closed bars) and detyrosinated tubulin (open bars) in COS cells transfected with MAP1B, GSK3β, or MAP1B and GSK3β (BOTH) as indicated. Equal quantities of protein from different samples were prepared for SDS-PAGE and immunoblotted with mAB TAT-1, mAb YL1/2 and pAb SUP GLU. Probing duplicate blots with mAb SMI-31 indicated that COS cells transfected with MAP1B and GSK3β expressed on average eight times more MAP1B-P than cells transfected with MAP1B alone (not shown and see Fig. 1). The results are densitometric measurements normalised to the values for control cells. Results are mean ± s.e.m. from four, independent experiments.

Table 1. Effect of nocodazole on microtubules in transfected COS cells

	Transfection	
Category	MAP1B	MAP1B/GSK3β
Background microtubule numbers (mean ± s.e.m.%)	13.9±1.8	61.9±2.9
Medium microtubule numbers (mean ± s.e.m.%)	17.3±4.7	8.7±2.9
High microtubule numbers (mean ± s.e.m.%)	68.8±4.1	29.4±1.8

The microtubule content of COS cells transfected with MAP1B, or MAP1B and GSK3β and then treated with nocodazole was examined. COS cells transfected with MAP1B cDNA and expressing high levels of protein show an increased microtubule content compared to untransfected cells. In contrast, COS cells transfected with MAP1B and GSK3β, which express high levels of MAP1B-P, do not show an increase in microtubule numbers. In MAP1B transfections approximately 16% of cells that express MAP1B, also express MAP1B-P (generated by endogenous GSK3β kinase activity). In double transfections, about 70% of the cells that express MAP1B also express MAP1B-P (i.e. 30% of cells express MAP1B). These figures correlate well with the proportion of transfected cells that show resistance to nocodazole treatment and are in close agreement with the immunoblotting data presented in Fig. 1.

relationship between MAP1B-P and detyrosinated microtubules by quantifying fluorescence intensity of pAb SUP GLU staining and comparing it with MAP1B and MAP1B-P in individual transfected COS cells from cultures transfected either with MAP1B alone or MAP1B and GSK3β (Fig. 3C). These results suggest that expression of high levels of MAP1B-P in COS and CHO cells causes a loss of detyrosinated, but not acetylated microtubules.

In confirmation of the immunofluorescence experiments, immunoblotting experiments showed that there was a reduction in the levels of detyrosinated α-tubulin in double transfected cultures compared to controls (Fig. 4). The biochemical changes observed were relatively small, probably reflecting the fact that only a proportion of cells become transfected.

MAP1B, but not MAP1B-P, protects microtubules against nocodazole depolymerisation

Previous work has shown that transfection of COS cells with MAP1B protects microtubules against depolymerisation by nocodazole (Takemura et al., 1992). We also examined the effects of MAP1B transfection on microtubule depolymerisation by nocodazole. In control COS cell cultures, nocodazole treatment caused the loss of tyrosinated microtubules and a reduction in detyrosinated microtubules in the majority of cells (not shown). In contrast, in MAP1B transfected COS cell cultures, cells expressing high levels of MAP1B retained microtubules after nocodazole treatment (Fig. 5A), confirming earlier observations (Takemura et al., 1992). However, after transfection with MAP1B and GSK3β, far fewer cells had microtubules, particularly those cells with high levels of MAP1B-P (Fig. 5B). Cotransfection of MAP1B and GSK3β led to a large decrease in the number of MAP1B expressing cells retaining microtubules after nocodazole treatment, down to 30% from 70% (Table 1). This level of protection may reflect the proportion of cells in double transfections that express unphosphorylated MAP1B (approx. 30%, see Table 1). The level of protection in single transfections (14% of cells contain background levels of microtubules) may also reflect the proportion of MAP1B transfected cells that express MAP1B-P (16%). These data suggest that phosphorylation of MAP1B by GSK3β reduces or abolishes the ability of MAP1B to protect microtubules against nocodazole depolymerisation.

MAP1B binds to tyrosinated, but not to detyrosinated, microtubules independently of phosphorylation

To help to understand the mechanism by which MAP1B-P controls microtubule stability we need to ascertain the effect of phosphorylation on microtubule interactions. To investigate this question, we detergent extracted MAP1B transfected COS cell cultures, to separate soluble proteins from the insoluble cytoskeleton (Bush et al., 1996). Biochemical analysis of the soluble and cytoskeletal fractions confirmed that MAP1B associates with the cytoskeleton (Fig. 6). Interestingly, the proportion of total MAP1B associating with the cytoskeleton was unchanged by GSK3β co-transfection, indicating that phosphorylation by this kinase has no significant effect on the microtubule binding affinity of MAP1B (Fig. 6, MAP1B, P, and BOTH, P). Similar partitioning is shown by MAP1B-P (not shown). Quantitative analysis of immunoblots showed that 34% (average of three experiments) of the total MAP1B is present in the cytoskeleton in MAP1B transfected COS cells and 37% (average of three experiments) of MAP1B is present in the cytoskeleton in double transfected cells. Immunoblotting showed that GSK3β also associates with the cytoskeleton (Fig. 6, BOTH, S and BOTH, P). Immunofluorescence of detergent extracted cultures stained with GSK3β antibodies revealed that GSK3β binds to microtubules in COS cells (not shown), confirming earlier observations (Mandelkow et al., 1992). Immunoblot analysis of the distribution of tyrosinated α-tubulin, which is associated with unstable microtubules, and

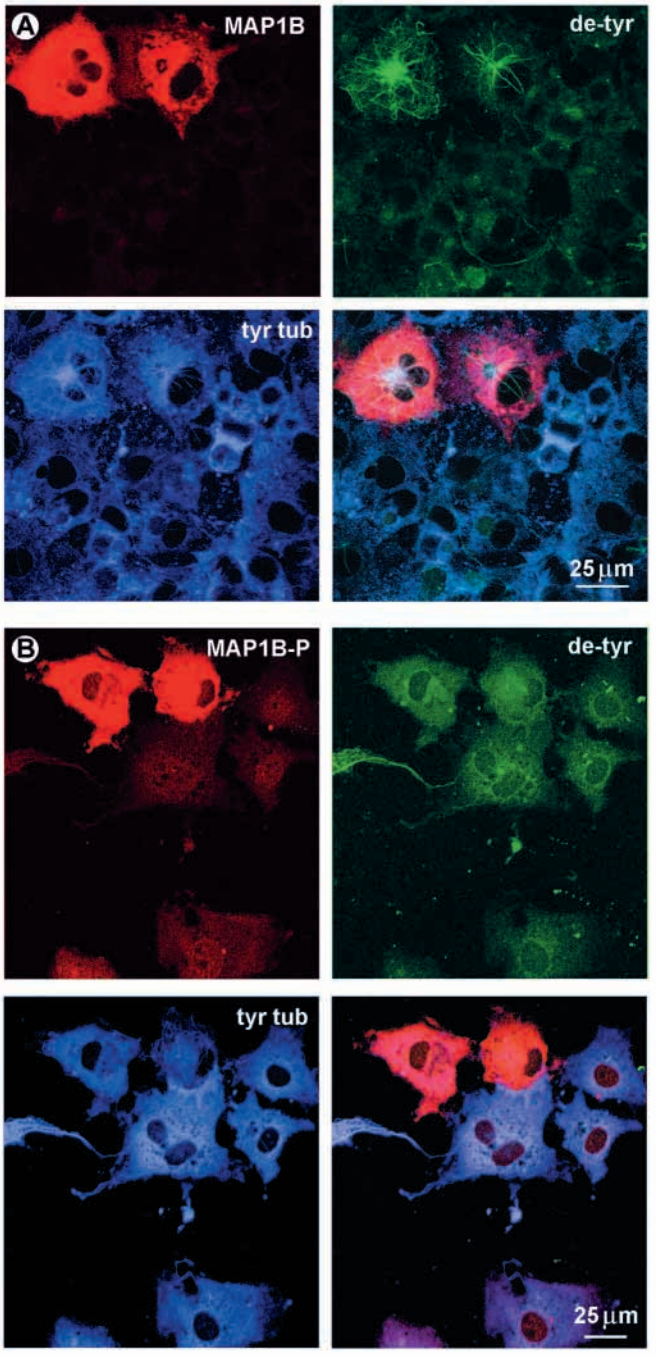

Fig. 5. MAP1B, but not MAP1B-P, protects microtubules against nocodazole depolymerisation. (A) Transfection of COS cells with MAP1B protects microtubules against nocodazole depolymerisation. Confocal fluorescence images of COS cells transfected with MAP1B and triple labelled with mAb R which labels MAP1B (red), pAb SUP GLU (green), which labels detyrosinated microtubules, and mAb YL 1/2 (blue), which labels tyrosinated microtubules. The cells were treated with nocodazole (0.1 μg/ml) for 30 minutes. In cells which express high levels of MAP1B (red), microtubules are preserved (green and blue), whereas untransfected cells have few or no microtubules. (B) Confocal fluorescence images of COS cells transfected with MAP1B and GSK3β and triple labelled with mAb SMI-31, which labels MAP1B-P (red), pAb SUP GLU (green), which labels detyrosinated microtubules, and mAb YL 1/2 (blue), which labels tyrosinated microtubules. The cells were treated with nocodazole (0.1 μg/ml) for 30 minutes. The expression of high levels of MAP1B-P (red) does not protect cells against the microtubule depolymerising action of nocodazole. Tyrosinated microtubules (blue) are lost from these cells. Note also the lack of detyrosinated microtubules (green, c.f. A, de-tyr).

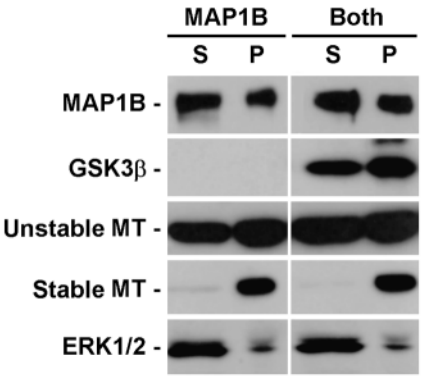

Fig. 6. Phosphorylation of MAP1B by GSK3β does not alter its association with the cytoskeleton. Biochemical analysis of the distribution of MAP1B, tubulin, GSK3β and ERK1 and 2 in transfected COS cells. Cytosolic (S) and cytoskeletal (P) fractions were prepared from equal amounts of MAP1B (MAP1B) and double transfected (Both) cells. Double transfection does not affect the distribution of MAP1B or stable/unstable microtubules between the cytosol and the cytoskeleton. Note the association of some GSK3β with the cytoskeleton, as compared to the distribution of ERK1 and 2 which is almost completely soluble in these cells.

de-tyrosinated α-tubulin, associated with stable microtubules, showed that there was no change in the partitioning of these isoforms of tubulin between the cytoskeleton and soluble pool in double transfected COS cells compared with cells transfected with MAP1B alone (Fig. 6). These observations indicate that a change in microtubule affinity cannot explain the effect of MAPIB-P on microtubule stability.

To investigate the mechanism of action further we detergent extracted MAP1B transfected COS cells, to remove soluble proteins and preserve the cytoskeleton (Bush et al., 1996), and then triple labelled the cultures with mAb YL 1/2, pAb SUP GLU and a monoclonal antibody that recognises all isoforms of MAP1B independent of their phosphorylation (mAb R, Riederer et al., 1986). Under these conditions all MAP1B staining is filamentous and co-localised with tyrosinated, but not with detyrosinated microtubules (Fig. 7A). This finding suggests that MAP1B cannot bind to detyrosinated microtubules. To determine whether MAP1B can bind to acetylated microtubules we performed double labelling experiments with mAb 6-11B-1, which recognises acetylated tubulin (Piperno and Fuller, 1985) and a pAb to MAP1B (αMAP1B-C1, Johnstone et al., 1997b). This showed that MAP1B binds to the majority of acetylated microtubules but not to a sub-population that are characteristically highly curled (Fig. 7B). In double transfected cells, MAP1B-P binds to tyrosinated microtubules, but, in the small proportion of cells which retain a few detyrosinated microtubules, MAP1B-P does not bind to detyrosinated microtubules (not shown). Since most detyrosinated microtubules are highly curled (Fig. 3), we

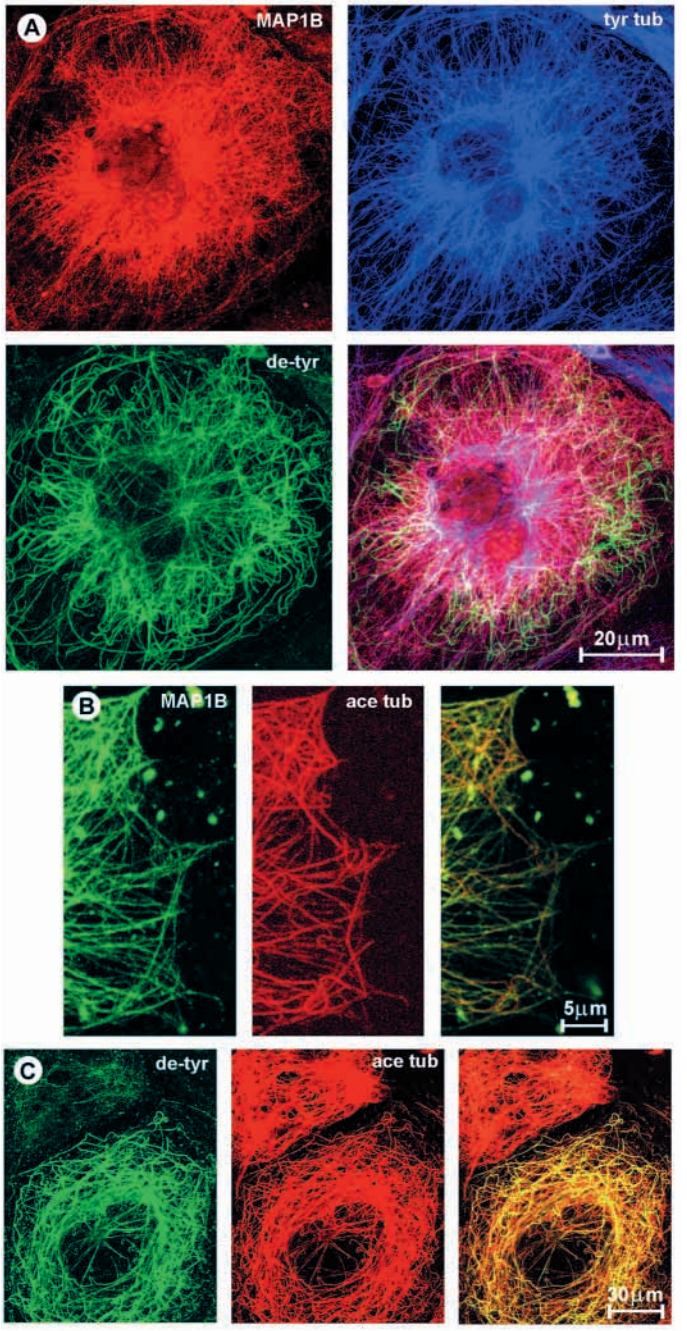

Fig. 7. (A) MAP1B can bind to tyrosinated, but not to detyrosinated microtubules. COS cell cultures transfected with MAP1B were detergent extracted, to preserve the cytoskeleton and remove soluble proteins, and then triple labelled with mAb R (red), which recognises all isoforms of MAP1B, mAb YL 1/2 (blue), which labels tyrosinated microtubules, and pAb SUP GLU (green), which labels detyrosinated microtubules. Staining for MAP1B (red) is clearly filamentous and most closely co-localised with tyrosinated microtubules (blue). This is confirmed in the merged triple images in which the colour of the detyrosinated microtubules remains unchanged (green) whereas the tyrosinated microtubules have become mauve, due to an overlap of the blue and red fluorescence. (B) MAP1B binds to a sub-population of acetylated microtubules. COS cell cultures transfected with MAP1B were detergent extracted, to preserve the cytoskeleton and remove soluble proteins, and then double labelled with a pAb to MAP1B (αMAP1B-C1, green) and mAb 6-11B-1 (red), which recognises acetylated microtubules. The MAP1B antibody labels the majority of the acetylated microtubules except for a sub-population of highly curled microtubules, as confirmed in the merged images. (C) Detyrosinated microtubules are almost co-extensive with the acetylated microtubules. COS cells were double labelled with pAb SUP GLU (green) to identify detyrosinated microtubules, and mAb 6-11B-1 (red) to identify acetylated microtubules. Most of the detyrosinated microtubules are highly curled and are almost co-extensive with the acetylated microtubules. Note that one cell in the field contains abundant acetylated microtubules but very few detyrosinated microtubules.

investigated the possibility that the sub-population of acetylated microtubules that MAP1B did not bind to were detyrosinated. To do this we double labelled COS cells with mAb 6-11B-1 and pAb SUP GLU and found that detyrosinated microtubules are almost co-extensive with the acetylated microtubules in these cells (Fig. 7C). However, the small population of COS cells that completely lack detyrosinated microtubules have many acetylated microtubules (Fig. 7C).

Reduction of MAP1B-P levels in dorsal root ganglion cell cultures dramatically increases detyrosinated microtubules

Dissociated dorsal root ganglion cells from early postnatal mice rapidly extend axons in culture and by 24 hours have produced a branching network of long, thin axons tipped with small growth cones (Fig. 8A). When these neurons first extend axons, during the first few hours of culture, the growth cones are much larger (A, inset). In striking contrast, when cultured for 24 hours in the presence of 10 mM LiCl, dorsal root ganglion cells have stunted axons which are far thicker than normal and are tipped with giant growth cones (Fig. 8B). These giant growth cones are similar in size to those seen in untreated, younger cultures (A, inset). Similar morphological changes were seen in cerebellar granule cell cultures treated with lithium (Lucas et al., 1998). In control cultures, labelling with antibodies against unstable (tyrosinated) and stable (detyrosinated) microtubules showed that the unstable microtubules are present within the growth cone whereas the stable microtubules are restricted to more proximal locations near the axon (Fig. 8A and inset). In contrast, in lithium-treated cultures, stable microtubules are distributed throughout the giant growth cones and extend as far distally as the unstable microtubules (Fig. 8B, c.f. A, inset). Within these growth cones, the numbers of stable microtubules is far greater than in control cultures. Immunoblotting analysis of dorsal root ganglion cell cultures showed that there was a small decline in the amount of total tubulin in lithium treated cultures but a large increase in the relative amount of stable (detyrosinated) tubulin (not shown), confirming the immunofluorescence observations. Immunoblotting also revealed a dramatic decline in the amount of MAP1B-P in lithium-treated cultures (not shown), in agreement with our previous observations with cerebellar granule cell cultures (Lucas et al., 1998).

DISCUSSION

We have recently shown that the proline-directed serine/threonine kinase GSK3β (Woodgett, 1990)

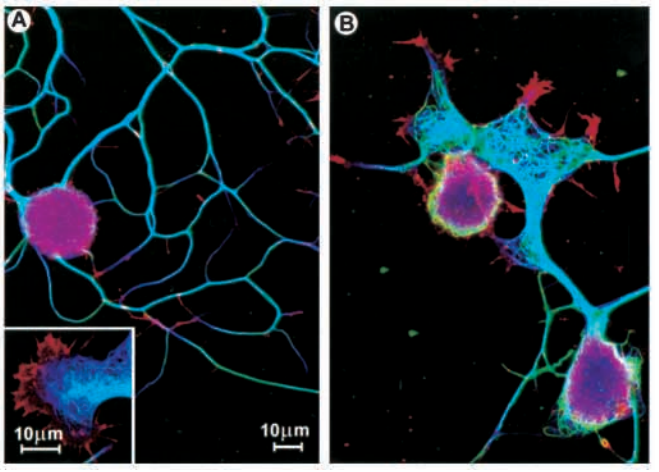

Fig. 8. (A) Dorsal root ganglion cell cultured for 24 hours in medium supplemented with 10 mM NaCl. The neuron has been labelled with mAb AC15, which labels β-actin (red), mAb YL1/2, which labels tyrosinated microtubules (blue), and pAb SUP GLU, which labels detyrosinated microtubules (green). After 24 hours in culture the neuron has extended a system of highly branched axons tipped with small growth cones. Note that the tyrosinated microtubules (blue) extend more distally that the detyrosinated microtubules (green). Turquoise indicates the co-localisation of tyrosinated and detyrosinated microtubules. Inset: High power view of a growth cone from a 9 hr culture showing the more distal location of tyrosinated microtubules (blue) compared to detyrosinated microtubules (green). Turquoise indicates the co-localisation of tyrosinated and detyrosinated microtubules. (B) A dorsal root ganglion cell from a culture treated with 10 mM LiCl for 24 hours and stained as in A. Although the neuron has extended a system of axons many are shorter and thicker than normal and end in giant growth cones (c.f. A). These growth cones are larger than those seen in younger cultures (A, inset). Characteristically, the giant growth cones are filled with highly curled, detyrosinated microtubules. Turquoise indicates the co-localisation of tyrosinated and detyrosinated microtubules. Magnification as in A.

phosphorylates MAP1B in vitro and in neonatal mouse cerebellar granule cells in culture (Lucas et al., 1998). The phosphorylation site maps to a region of MAP1B that contains a high concentration of SP motifs and is recognised by mAb SMI-31 (Johnstone et al., 1997a). The double transfection experiments with MAP1B and GSK3β reported here confirm that MAP1B is a substrate for GSK3β at a site recognised by mAb SMI-31. Furthermore, we also showed that lithium, an inhibitor of GSK3β (Klein and Melton, 1996; Stambolic et al., 1996; Hedgepeth et al., 1997), blocked the phosphorylation of MAP1B by GSK3β in double transfected cells. In addition, we found that cells expressing high levels of MAP1B phosphorylated by GSK3β (MAP1B-P) had few or no detyrosinated microtubules, as indicated by a lack of staining with pAb SUP GLU, which recognises detyrosinated microtubules (Gundersen et al., 1984; Piperno et al., 1987). Acetylated microtubules were not lost. This finding was confirmed by immunoblotting. Importantly, the loss of detyrosinated microtubules in double transfected cell cultures was blocked by treatment with lithium. We also found that MAP1B can protect microtubules against nocodazole depolymerisation, a result which confirms previous findings (Takemura et al., 1992), and further showed that phosphorylation of MAP1B by GSK3β abolishes this protective effect. In addition, we showed that MAP1B can bind to tyrosinated microtubules but not to detyrosinated microtubules and that this binding is unaffected by GSK3β phosphorylation. Collectively, these results suggest that MAP1B can affect the stability of microtubules and that this can be regulated by GSK3β phosphorylation of MAP1B.

In previous MAP1B transfection experiments in non-neuronal cells it was found that although microtubules were stabilised against drug-mediated disassembly, they were not bundled (Noble et al., 1989; Takemura et al., 1992). We also did not detect any changes in microtubule bundling in MAP1B transfected COS cells. Takemura et al. (1992) also found that MAP1B transfection of COS cells increased the numbers of acetylated microtubules but did not affect detyrosinated microtubules. We found that MAP1B transfection of COS cells slightly decreased detyrosinated microtubules and that acetylated microtubules remained unchanged or increased. In addition, we found that when transfected MAP1B was phosphorylated by co-transfection with GSK3β, the resulting high levels of expression of MAP1B-P was associated with a loss of detyrosinated microtubules but that acetylated microtubules were not lost. Stable microtubules are formed from existing unstable microtubules by a process which is poorly understood but which correlates with the conversion of the tyrosinated α-tubulin in these microtubules into detyrosinated and acetylated α-tubulin (Piperno et al., 1987; Schulze and Kirschner, 1987; Khawaja et al., 1988; reviewed by Wordeman and Mitchison, 1994). The detyrosination is catalysed by tyrosine carboxypeptidase, a tubulin-specific enzyme (Barra et al., 1973; Raybin and Flavin, 1977; Argarana et al., 1978; Kumar and Flavin, 1981) but is not causal to microtubule stability (Khawaja et al., 1988). Therefore, antibody markers to these post-translational modifications may not reflect changes in microtubule stability. Significantly, however, we found that MAP1B, phosphorylated by GSK3β, abrogated the protective effect of MAP1B against nocodazole-mediated microtubule depolymerisation, suggesting that MAP1B phosphorylation acts as a molecular switch to regulate microtubule stability.

MAP1B is phosphorylated at a number of sites and by at least two kinase classes: casein kinase II (Díaz-Nido et al., 1988) and proline-directed serine/threonine kinases (DiTella et al., 1996; Lucas et al., 1998). The effects of individual phosphorylation sites on the properties of the molecule are not known although there is a general consensus that MAP1B isoforms phosphorylated by casein kinase II bind to microtubules more effectively than unphosphorylated isoforms (Aletta et al., 1988; Brugg and Matus, 1988; Díaz-Nido et al., 1988; Ulloa et al., 1993a). In the present experiments, we found evidence that GSK3β phosphorylation of MAP1B is involved in the regulation of microtubule dynamics but we found no evidence to suggest that phosphorylation of MAP1B by GSK3β altered the affinity of MAP1B for microtubules. Therefore, our results suggest that different phosphorylation sites from those generated by GSK3β are involved in regulating the microtubule interactions of MAP1B.

What is the mechanism underlying the loss of detyrosinated microtubules from cells expressing high levels of MAP1B-P? Bulinski et al. (1988) showed that the population of

detyrosinated microtubules overlapped the population of acetylated microtubules in TC-7 cells. We found that in COS cells the population of detyrosinated microtubules is almost co-extensive with the acetylated microtubules. Bulinski et al. (1988) also showed that following recovery from nocodazole depolymerisation, acetylated microtubules form before detyrosinated microtubules. Collectively, these findings suggest that a sub-population of unstable microtubules first become acetylated and then, at a later time, detyrosinated. This is consistent with our observation that in COS cells lacking detyrosinated microtubules there are abundant acetylated microtubules (Fig. 7C). The cellular factors responsible for altering microtubule stability are unknown but MAPs are strong candidates. Since all MAP1B (Fig. 7A), and probably MAP1B-P, binds to tyrosinated microtubules but not to detyrosinated microtubules, MAP1B-P may cause the loss of detyrosinated microtubules indirectly by preventing their formation from tyrosinated microtubules. Pre-existing detyrosinated microtubules would then be lost by normal turnover and not replaced. In our experiments, COS cells were examined two days after transfection and therefore there is sufficient time for loss of stable microtubules by normal turnover (Schulze and Kirschner, 1987). MAP1B probably binds to the C-terminus of α/β-tubulin, precisely where this post-translational modification of tubulin occurs (Avila, 1991; Maccione and Cambiazo, 1995). This activity of MAP1B-P is not regulated simply by its association with microtubules, because GSK3β phosphorylation of MAP1B had no apparent effect on the microtubule binding of MAP1B (Fig. 6).

In developing neurons, the highest levels of phosphorylated MAP1B are found in growth cones, implying that phosphorylated MAP1B plays a role in growth cone function (Mansfield et al., 1991; Ulloa et al., 1994; Black et al., 1994; Bush and Gordon-Weeks, 1994; Bush et al., 1996; DiTella et al., 1996). Our finding that high levels of MAP1B-P expression in COS cells correlates with a loss of detyrosinated microtubules and a loss of protection of microtubules against nocodazole depolymerisation, suggests that a primary role of MAP1B-P in growing axons and growth cones may be to maintain microtubules in a dynamically unstable state. A singular feature of growth cone microtubules is that the majority are dynamically unstable and spread throughout the growth cone, whereas the small population of stable microtubules is proximally restricted (e.g. Fan et al., 1993; Williamson et al., 1996; Fig. 8A and inset). This is of functional significance because there appears to be a requirement for dynamically unstable microtubules in growth cone pathfinding (Tanaka et al., 1995; Williamson et al., 1996; Challacombe et al., 1997; reviewed by Tanaka and Kirschner, 1995).

If MAP1B-P maintains microtubules in growing axons and growth cones in a dynamic state then we would predict that loss of MAP1B-P would produce an increase in the number of detyrosinated microtubules in growing axons and growth cones. Therefore, we re-examined the effect of lithium treatment on neurons. We found that lithium treatment of dorsal root ganglion cells produced a down-regulation of MAP1B-P and similar morphological effects to that seen previously in cerebellar granule cells (Lucas et al., 1998); axons were shorter and thicker and growth cones were greatly enlarged. In addition, as predicted, we observed a marked increase in the number of detyrosinated microtubules in growth cones. This result is consistent with our proposal that MAP1B-P regulates microtubule stability in growing axons and growth cones. In a recent study of the effects of purified porcine brain MAP1B on microtubule dynamics it was found that MAP1B, unlike MAP2, does not reduce microtubule dynamic instability (Vandecandelaere et al., 1996). Since the purified MAP1B used in this study was phosphorylated at both casein kinase II and proline-directed serine/threonine sites, as is MAP1B found in growth cones, the implication of this study and our findings is that the presence of MAP1B-P in growth cones maintains a dynamic population of microtubules. However, it is not clear how the changes in microtubule stability relate to the observed morphological phenotype in lithium treated cultures. Growing axons are known to have higher levels of unstable microtubules than mature axons and this may relate to the shorter and thicker axons in the lithium treated cultures. Why these neurons have giant growth cones is less clear. There are other cytoskeletal target substrates for GSK3β in cells, including adenomatous polyposis coli protein (APC) and tau, and these substrates may also contribute to the observed phenotype. APC binds to microtubules and is concentrated in growth cones, but whether GSK3β phosphorylation modulates microtubule binding is not known (Morrison et al., 1997). Tau promotes microtubule assembly and bundling and GSK3β phosphorylation of tau causes a reduction in its ability to bundle microtubules (Wagner et al., 1996), whereas a reduction in tau phosphorylation caused by inhibition of GSK3β leads to an increase in microtubule binding (Hong et al., 1997; but see Utton et al., 1997) and promotion of microtubule assembly (Hong et al., 1997; Utton et al., 1997), which may lead to increased microtubule stability. Thus, some aspects of the effects of lithium treatment on cerebellar granule cells and dorsal root ganglion cells may relate to these other GSK3β substrates and we are currently studying these molecules to dissect out their contribution.

We particularly thank Phil Marsh for help with cDNA constructs, Rejith Dayanandan for help with transfections, Kate Kirwan for photography and graphic work, and Louise Cramer and Jean-Marc Gallo for critically reading the manuscript. GSK3β cDNA was a kind gift from Dr J. Woodgett and mouse MAP 1B cDNA was a kind gift from Prof. N. Cowan (Noble et al., 1989). We thank Dr J. C. Bulinski for pAb SUP GLU, Dr G. Piperno for mAb 6-11B-1 and Dr A. Matus for mAb R. This work was supported by the MRC, The Wellcome Trust and the Central Research Fund of London University. Rebecca Owen is supported by a BBSRC studentship.

REFERENCES

Aletta, J. M., Lewis, S. A., Cowan, N. J. and Greene, L. A. (1988). Nerve growth factor regulates both the phosphorylation and steady-state levels of microtubule associated protein 1. 2 (MAP 1. 2). *J. Cell Biol.* **106**, 1573-1581.

Argarana, C. E., Barra, H. S. and Caputto, R. (1978). Release of [^{14}C]-tyrosine from tubilinyl-[^{14}C]-tyrosine by brain extract. Separation of a carboxypeptidase from tubulin tyrosine ligase. *Mol. Cell Biochem.* **19**, 17-22.

Avila, J. (1991). Does MAP1B bind to tubulin through the interaction of α-helices? *Biochem. J.* **274**, 621-622.

Barra, H. S., Rodriguez, J. A., Arce, C. A. and Caputto, R. (1973). A soluble preparation from rat brain that incorporates into its own proteins [^{14}C] arginine by a ribonuclease-sensitive system and [^{14}C]-tyrosine by a ribonuclease-insensitive system. *J. Neurochem.* **20**, 97-108.

Black, M. M., Slaughter, T. and Fischer, I. (1994). Microtubule-associated protein 1b (MAP1b) is concentrated in the distal region of growing axons. *J. Neurosci.* **14**, 857-870.

Bloom, G. S., Luca, F. C. and Vallee, R. B. (1985). Microtubule-associated protein 1B: Identification of a major component of the neuronal cytoskeleton. *Proc. Nat. Acad. Sci. USA* **82**, 5404-5408.

Brugg, B. and Matus, A. (1988). PC12 cells express juvenile microtubule-associated proteins during nerve growth factor-induced neurite outgrowth. *J. Cell Biol.* **107**, 643-650.

Brugg, B., Reddy, D. and Matus, A. (1993). Attenuation of microtubule-associated protein 1B expression by antisense oligodeoxynucleotides inhibits initiation of neurite outgrowth. *Neuroscience* **52**, 489-496.

Bulinski, J. C., Richards, J. E. and Piperno, G. (1988). Posttranslational modifications of α-tubulin: Detyrosination and acetylation differentiate populations of interphase microtubules in cultured cells. *J. Cell Biol.* **106**, 1213-1220.

Bush, M. S. and Gordon-Weeks, P. R. (1994). Distribution and expression of developmentally regulated epitopes on MAP 1B and neurofilament proteins in the developing rat spinal cord. *J. Neurocytol.* **23**, 682-698.

Bush, M. S., Goold, R. G., Moya, F. and Gordon-Weeks, P. R. (1996). An analysis of an axonal gradient of phosphorylated MAP 1B in cultured sensory neurons. *Eur. J. Neurosci.* **8**, 235-248.

Calvert, R. and Anderton, B. H. (1985). A microtubule associated protein MAP 1 which is expressed at elevated levels during development of rat cerebellum. *EMBO J.* **4**, 1171-1176.

Challacombe, J. F., Snow, D. M. and Letourneau, P. C. (1997). Dynamic microtubule ends are required for growth cone turning to avoid an inhibitory guidance cue. *J. Neurosci.* **17**, 3085-3095.

DiTella, M. C., Feiguin, F., Carri, N., Kosik, K. S. and Cáceres, A. (1996). MAP-1B/TAU functional redundancy during laminin-enhanced axonal growth. *J. Cell Sci.* **109**, 467-477.

Díaz-Nido, J., Serrano, L., Méndez, E. and Avila, J. (1988). A casein kinase II-related activity is involved in phosphorylation of microtubule-associated protein MAP1B during neuroblastoma cell differentiation. *J. Cell Biol.* **106**, 2057-2065.

Edelmann, W., Zervas, M., Costello, P., Roback, L., Fischer, I., Hammarback, J. A., Cowan, J., Davies, P., Wainer, B. and Kucherlapati, R. (1996). Neuronal abnormalities in microtubule-associated protein 1B mutant mice. *Proc. Nat. Acad. Sci. USA* **93**, 1270-1275.

Fan, J., Mansfield, S. G., Redmond, T., Gordon-Weeks, P. R. and Raper, J. (1993). The organization of F-actin and microtubules in growth cones exposed to a brain-derived collapsing factor. *J. Cell Biol.* **121**, 867-878.

Fischer, I. and Romano-Clarke, G. (1990). Changes in microtubule-associated protein MAP1B phosphorylation during rat brain development. *J. Neurochem.* **55**, 328-333.

Fischer, I. and Romano-Clarke, G. (1991). Association of microtubule associated protein (MAP 1B) with growing axons in cultured hippocampal neurons. *Mol. Cell. Neurosci.* **2**, 39-51.

Goold, R. G. and Gordon-Weeks, P. R. (1998). Glycogen synthase kinase 3β phosphorylation of MAP1B: A switch regulating microtubule dynamics in the growth cone. Abstr. Am. Soc. Cell Biol., San Francisco, USA.

Gordon-Weeks, P. R., Mansfield, S. G., Alberto, C., Johnstone, M. and Moya, F. (1993). Distribution and expression of a phosphorylation epitope on MAP 1B that is transiently expressed in growing axons in the developing rat nervous system. *Eur. J. Neurosci.* **5**, 1302-1311.

Gordon-Weeks, P. R. (1997). MAPs in growth cones. In *Brain Microtubule Proteins: Modifications in Alzheimer's Disease.* (ed. J. Avila and K. Kosik), pp. 53-72. Harwood Academic Publishers.

Gundersen, G. G., Kalnoski, M. H. and Bulinski, J. C. (1984). Distinct populations of microtubules: tyrosinated and nontyrosinated alpha-tubulins are distributed differently *in vivo*. *Cell* **38**, 779-789.

Hedgepeth, C. M., Conrad, L. J., Zhang, J., Huang, H. C., Lee, V. M. Y. and Klein, P. S. (1997). Activation of the Wnt signalling pathway: A molecular mechanism for lithium action. *Dev. Biol.* **185**, 82-91.

Hong, M., Chen, D. C. R., Klein, P. S. and Lee, V. M. Y. (1997). Lithium reduces tau phosphorylation by inhibition of glycogen synthase kinase-3. *J. Biol. Chem.* **272**, 25326-25332.

Johnstone, M., Goold, R. G., Bei, D., Fischer, I. and Gordon-Weeks, P. R. (1997a). Localisation of microtubule-associated protein 1B phosphorylation sites recognised by monoclonal antibody SMI-31. *J. Neurochem.* **69**, 1417-1424.

Johnstone, M., Goold, R. G., Fischer, I. and Gordon-Weeks, P. R. (1997b). The neurofilament antibody RT97 recognises a developmentally regulated phosphorylation epitope on microtubule-associated protein 1B. *J. Anat.* **191**, 229-244.

Khawaja, S., Gundersen, G. F. and Bulinski, J. C. (1988). Enhanced stability of microtubules enriched in detyrosinated alpha-tubulin is not a direct function of detyrosination level. *J. Cell Biol.* **106**, 141-149.

Kilmartin, J. V., Wright, B. and Milstein, D. (1982). Rat monoclonal antitubulin antibodies derived by using as new non-secretory rat cell line. *J. Cell Biol.* **93**, 576-582.

Klein, P. S. and Melton, D. A. (1996). A molecular mechanism for the effect of lithium on development.*Proc. Nat. Acad. Sci. USA* **93**, 8455-8459.

Kumar, N. and Flavin, M. (1981). Preferential action of a brain detyrosinolated carboxypeptidase on polymerised tubulin. *J. Biol. Chem.* **256**, 7678-7686.

Kutschera, W., Zauner, W., Wiche, G. and Propst, F. (1998). The mouse and rat MAP1B genes: Genomic organization and alternative transcription. *Genomics* **49**, 430-436.

Laemmli, U. K. (1970). Cleavage of structural proteins during the assembly of the head of bacteriophage T4. *Nature* **227**, 680-685.

Lovestone, S., Reynolds, H. C., Latimer, D., Davis, D. R., Anderton, B. H., Gallo, J.-M., Hanger, D., Mulot, S., Marquardt, B., Stabel, S., Woodgett, J. R. and Miller, C. C. J. (1994). Alzheimer's disease-like phosphorylation of the microtubule-associated protein tau by glycogen synthase kinase-3 in transfected mammalian cells. *Curr. Biol.* **4**, 1077-1086.

Lucas, F. R., Goold, R. G., Gordon-Weeks, P. R. and Salinas, P. C. (1998). Inhibition of GSK-3β leading to the loss of phosphorylated MAP-1B is an early event in axonal remodelling induced by WNT-7a or lithium. *J. Cell Sci.* **111**, 1351-1361.

Maccione, R. B. and Cambiazo, V. (1995). Role of microtubule-associated proteins in the control of microtubule assembly. *Physiol. Revs.* **75**, 835-864.

Mandelkow, E.-M., Drewes, G., Biernat, J., Gustke, N., van Lint, J., van Denheede, J. R. and Mandelkow, E. (1992). Glycogen synthase kinase-3 and the Alzheimer's diseasae-like state of microtubule-associated protein tau. *FEBS Lett.* **314**, 315-321.

Mansfield, S. G., Diaz-Nido, J., Gordon-Weeks, P. R. and Avila, J. (1991). The distribution and phosphorylation of the microtubule-associated protein MAP 1B in growth cones. *J. Neurocytol.* **21**, 1007-1022.

Morrison, E. E., Askham, J., Clissold, P., Markham, A. F. and Meredith, D. M. (1997). Expression of beta-catenin and the adenomatous polyposis coli tumour suppressor protein in mouse. *Neurosci. Letts.* **235**, 129-132.

Müller, R., Kindler, S. and Garner, C. C. (1994). The MAP1 family. In *Microtubules* (ed. J. S. Hyams and C. W. Lloyd), pp. 141-154. Wiley-Liss, Inc., New York.

Noble, M., Lewis, S. A. and Cowan, N. (1989). The microtubule binding domain of the microtubule-associated protein MAP-1B contains a repeated sequence motif unrelated to that of MAP-2 and tau. *J. Cell Biol.* **109**, 3367-3376.

Pedrotti, B. and Islam, K. (1996). Dephosphorylated but not phosphorylated microtubule associated protein MAP1B binds to microfilaments. *FEBS Lett.* **388**, 131-133.

Piperno, G. and Fuller, M. T. (1985). Monoclonal antibodies specific for an acetylated form of α-tubulin recognize the antigen in cilia and flagella from a variety of organisms. *J. Cell Biol.* **104**, 289-302.

Piperno, G., Ledizet, M. and Chang, X. (1987). Microtubules containing acetylated α-tubulin in mammalian cells in culture. *J. Cell Biol.* **104**, 289-302.

Raybin, D. and Flavin, M. (1977). Enzyme which specifically adds tyrosine to the α-chain of tubulin. *Biochemistry* **16**, 2189-2194.

Riederer, B., Cohen, R. and Matus, A. (1986). MAP 5: a novel microtubule associated protein under strong developmental regulation. *J. Neurocytol.* **15**, 763-775.

Sato-Yoshitake, R., Shiomura, Y., Miyasaka, H. and Hirokawa, N. (1989). Microtubule-associated protein 1B: Molecular structure, localization, and phosphorylation-dependent expression in developing neurons. *Neuron* **3**, 229-238.

Schliwa, M. and van Blerkom, J. (1981). Structural interaction of cytoskeletal components. *J. Cell Biol.* **90**, 222-235.

Schoenfeld, T. A., McKerracher, L., Obar, R. and Vallee, R. B. (1989). MAP1A and MAP1B are structurally related microtubule associated proteins with distinct developmental patterns in the CNS. *J. Neurosci.* **9**, 1712-1730.

Schulze, E. and Kirschner, M. (1987). Dynamic and stable populations of microtubules in cells. *J. Cell Biol.* **97**, 1249-1254.

Stambolic, V., Ruel, L. and Woodgett, J. R. (1996). Lithium inhibits

glycogen synthase kinase-3 activity and mimics wingless signalling in intact cells. *Curr. Biol.* **6**, 1664.

Takei, Y., Kondo, S., Harada, A., Inomata, S., Noda, T. and Hirokawa, N. (1997). Delayed development of nervous system in mice homozygous for disrupted microtubule-associated protein 1B (MAP1B) gene. *J. Cell Biol.* **137**, 1615-1626.

Takemura, R., Okabe, S., Umeyama, T., Kanai, Y., Cowan, N. J. and Hirokawa, N. (1992). Increased microtubule stability and alpha tubulin acetylation in cells transfected with microtubule-associated proteins MAP-1B, MAP2 and tau. *J. Cell Sci.* **103**, 953-964.

Tanaka, E. and Kirschner, M. W. (1995). The role of microtubules in growth cone turning at substrate boundaries. *J. Cell Biol.* **128**, 127-137.

Tanaka, E., Ho, T. and Kirschner, M. W. (1995). The role of microtubule dynamics in growth cone motility and axonal growth. *J. Cell Biol.* **128**, 139-155.

Towbin, H., Staehlin, T. and Gordon, J. (1979). Electrophoretic transfer of proteins from polyacrylamide gels to nitrocellulose sheets: procedure and applications. *Proc. Nat. Acad. Sci. USA* **76**, 4350-4354.

Tucker, R. P., Binder, L. I. and Matus, A. (1988). Neuronal microtubule-associated proteins in the embryonic avian spinal cord. *J. Comp. Neurol.* **271**, 44-55.

Ulloa, L., Díaz-Nido, J. and Avila, J. (1993a). Depletion of casein kinase II by antisense oligonucleotide prevents neuritogenesis in neuroblastoma cells. *EMBO J.* **12**, 1633-1640.

Ulloa, L., Avila, J. and Díaz Nido, J. (1993b). Heterogeneity in the phosphorylation of microtubule-associated protein MAP 1B during rat brain development. *J. Neurochem.* **61**, 961-972.

Ulloa, L., Díez-Guerra, J., Avila, J. and Díaz-Nido, J. (1994). Localization of differentially phosphorylated isoforms of microtubule associated protein 1B (MAP1B) in cultured rat hippocampal neurons. *Neurosci.* **61**, 211-223.

Utton, M. A., Vandecandelaere, A., Wagner, U., Reynolds, C. H., Gibb, G. M., Miller, C. C. J., Bayley, P. M. and Anderton, B. H. (1997). Phosphorylation of tau by glycogen synthase kinase 3β affects the ability of tau to promote microtubule self-assembly. *Biochem. J.* **323**, 741-747.

Vandecandelaere, A., Pedrotti, B., Utton, M. A., Calvert, R. and Bayley, P. M. (1996). Differences in the regulation of microtubule dynamics by microtubule-associated proteins MAP1B and MAP2. *Cell Motil. Cytoskel.* **35**, 134-146.

Wagner, U., Utton, M. A., Gallo, J. M. and Miller, C. C. J. (1996). Cellular phosphorylation of tau by GSK-3beta influences tau binding to microtubules and microtubule organisation. *J. Cell Sci.* **109**, 1537-1543.

Wehland, J., Schroder, H. C. and Weber, K. (1984). Amino acid sequence requirements in the epitope recognised by the α-tubulin-specific rat monoclonal antibody YL 1/2. *EMBO J.* **3**, 1295-1300.

Williamson, T. W., Gordon-Weeks, P. R., Schachner, M. and Taylor, J. (1996). Microtubules are obligatory for growth cone turning. *Proc. Nat. Acad. Sci. USA* **93**, 15221-15226.

Woodgett, J. R. (1990). Molecular cloning and expression of glycogen synthase kinase-3/factor A. *EMBO J.* **9**, 2431-2438.

Woods, A., Sherwin, T., Sasse, R., MacRae, T. H., Baines, A. J. and Gull, K. (1989). Definition of individual components within the cytoskeleton of *Trypanosoma brucei* by a library of monoclonal antibodies. *J. Cell Sci.* **93**, 491-500.

Wordeman, L. and Mitchison, T. J. (1994). Dynamics of microtubule asembly *in vivo*. In *Microtubules* (ed. J. S. Hyams and C. W. Lloyd), pp. 287-301. Wiley-Liss, Inc., New York.